A molecular-dynamics simulation study of dielectric relaxation in a 1,4-polybutadiene melt

Grant D. Smith[a] and Oleg Borodin
Department of Materials Science and Engineering and Department of Chemical and Fuels Engineering, University of Utah, Salt Lake City, Utah 84112

Wolfgang Paul
Institut für Physik, Johannes Gutenberg Universität, Staudingerweg 7 D55099 Mainz, Germany

(Received 25 March 2002; accepted 10 September 2002)

We have carried out atomistic molecular dynamics simulations of a melt of 1,4-poly(butadiene) from temperatures well above the experimentally observed merging of the primary α process and secondary β process down to temperatures approaching the experimentally observed bifurcation temperature. The relaxation strength and maximum loss frequency and its temperature dependence for the combined α-β dielectric relaxation process from simulations were in good agreement with experiment. The maximum loss frequency, melt viscosity, chain normal-mode relaxation times and torsional autocorrelation times were found to exhibit nearly identical non-Arrhenius temperature dependencies well represented by a Vogel–Fulcher fit with parameters in good agreement with experimental values obtained from dielectric and viscosity measurements. The dielectric susceptibility showed increasing intensity at high frequency for the lower temperatures investigated, indicative of a breakdown in time-temperature superposition due to an emerging β process. Comparison of time scales for the chain normal-mode dynamics and dielectric relaxation revealed that the latter is associated with motions on the segmental length scale. The correspondence of time scales and temperature dependence for the dielectric relaxation and the torsional autocorrelation function further confirmed the localized nature of the dielectric relaxation and indicated that the combined α-β dielectric process is fundamentally tied to microscopic conformational dynamics of individual dihedrals. However, the mean conformational transition rates were found to exhibit Arrhenius temperature dependence, leading to a divergence of time scales between the torsional, dielectric, chain and mechanical relaxation processes and the rates of conformational transitions with decreasing temperature. This divergence was associated with the increasingly heterogeneous character of conformational dynamics in the melt with decreasing temperature. Hence, the time scale of the principal (α) relaxation in the melt is fundamentally correlated with the time scale for homogenization of conformational dynamics, and not to the time scale of the conformational transitions themselves. © *2002 American Institute of Physics.* [DOI: 10.1063/1.1518684]

I. INTRODUCTION

The relaxation behavior of polymers has long been the subject of intense experimental and theoretical study. As a result, our phenomenological understanding of relaxation processes in polymers has advanced considerably. It is now accepted that all glass-forming polymers exhibit at least one relaxation process in addition to the primary α relaxation.[1] This secondary, or β relaxation, also known as the Johari–Goldstein process,[2] splits from the α process in a temperature range 10% to 20% above the phenomenological glass transition temperature T_g.[3] At higher temperatures, relaxation appears to be due to a single combined α-β process. The α process exhibits dramatic increase in relaxation time around T_g. The β process, however, continues to be manifest well below the glass transition and typically exhibits Arrhenius temperature dependence. While the α process is believed to be related to segmental relaxations of the polymer chains and the β process is believed to be due to local motions, a fundamental mechanistic understanding of these relaxations lags far behind the well-developed phenomenological picture. The nature of the underlying molecular motions leading to the α, β, and α-β processes, and particularly the relationship between the secondary relaxation and primary relaxation, are largely unknown: Hence, relaxations in polymers remain topics of active experimental, simulation and theoretical studies.

1,4-polybutadiene (PBD), a random copolymer of 1,4-trans, 1,4-cis, and 1,2-vinyl repeat units, is an excellent model polymer for the study of relaxation behavior in glass forming polymers. Experimental techniques that have been applied in the study of the relaxation behavior of PBD include fluorescence anisotropy decay,[4] nuclear magnetic resonance (NMR) spin-lattice relaxation,[5–7] ultrasound,[8,9] dynamic mechanical spectroscopy,[10–12] and light scattering,[8,13–15] along with dielectric spectroscopy[3,12,15,16] and neutron scattering.[3,17–29] The extremely wide frequency range of dielectric spectroscopy makes this technique a very

[a]Electronic mail: gsmith2@gibbon.mse.utah.edu

powerful temporal probe. In this work we utilize atomistic molecular dynamics (MD) simulations to gain a better understanding of the temperature dependence of dielectric relaxation in a PBD melt in the combined α-β regime approaching the bifurcation temperature (T_b), below which separate dielectric α and β processes are experimentally resolvable. Additionally, we relate dielectric relaxation in PBD for $T > T_b$ to chain relaxation and the conformational transitions that are fundamentally responsible for the α, β and combined α-β relaxation processes in conformationally flexible polymers.

II. MODEL AND METHODOLOGY

The PBD melt system and the MD simulation methodology utilized in our simulation study of dielectric relaxation are described in detail in our recently published work.[30,31] Briefly, the system consists of 40 chains of 30 repeat units. The chains are random copolymers of 50% 1,4-trans, 40% 1,4-cis and 10% 1,2-vinyl units. The quantum chemistry based united atom potential[30,32] used in our PBD melt simulations has been fully validated by comparison of melt dynamics obtained from MD simulations with NSE measurements of the single chain dynamic structure factor,[30,33,34] ^{13}C NMR spin lattice relaxation,[30,31] and the dynamic shear modulus.[35–37] Excellent agreement with experiment has confirmed the ability of our PBD melt simulations to reproduce polymer dynamics on all time and length scales accessible to the simulations. In this work the MD simulations were utilized to investigate the dielectric and chain relaxation behavior as well as conformational dynamics of PBD melts over a very wide temperature range, specifically at 500, 450, 400, 353, 323, 293, 273, and 253 K, approaching the experimentally observed dielectric bifurcation temperature of $T_b \approx 210$ K (MW = 7600).[15] All trajectories except 500, 450, and 253 K were taken from our previous work[30,31] and were analyzed as described below. Additional simulations were performed for systems at 500, 450, and 253 K. An equilibrated system at 400 K was used as the starting configuration for the 500 and 450 K systems. NPT equilibration for several Rouse times was performed in order to determine the equilibrium density at these temperatures, followed by ~10 Rouse times of NVT simulation. The system at 253 K was obtained from the 273 K system by performing a 10 ns (several segmental relaxation times[38]) simulation in the NPT at the lower temperature. These systems were then simulated in the NVT ensemble for 20 ns at 450 and 500 K, and 120 ns at 253 K. NVT simulations were carried out in a cubic simulation cell using a Nose–Hoover thermostat[39] with multiple time step reversible reference system propagator algorithm[40] utilizing a 1 fs time step for intramolecular forces and a 4 fs time step for intermolecular forces. For all systems, no drift in pressure, energy, pair distribution functions, conformational populations or chain dimensions was observed during the NVT sampling simulations, indicating adequate structural and conformational equilibration.

III. DIELECTRIC RELAXATION

A. Calculation

Linear response theory allows us to obtain the complex dielectric permittivity $\epsilon^*(\omega) = \epsilon' + i\epsilon''$ for the PBD melt using the relationship[41]

$$\frac{\epsilon' + i\epsilon''}{\Delta\epsilon} = 1 - i\omega \int_0^\infty \Phi(t)\exp(-i\omega t)dt, \tag{1}$$

where the dipole moment autocorrelation function (DACF) is given by

$$\Phi(t) = \frac{\langle \mathbf{M}(0)\cdot\mathbf{M}(t)\rangle}{\langle \mathbf{M}(0)\cdot\mathbf{M}(0)\rangle}, \tag{2}$$

and the relaxation strength $\Delta\epsilon = \epsilon_r - \epsilon_u$ is given by[42,43]

$$\Delta\epsilon = \left(\frac{\epsilon_u + 2}{3}\right)^2 \frac{3\epsilon_r}{2\epsilon_r + \epsilon_u} \frac{\langle M(0)^2\rangle}{3V\epsilon_o kT}. \tag{3}$$

Here, $\mathbf{M}(t)$ is the dipole moment of the system at time t, V is the volume of the system, k_B is the Boltzmann constant and T is the temperature, while $\langle\rangle$ denotes an ensemble average. The unrelaxed dielectric constant ϵ_u is the dielectric constant that includes all relaxation processes at frequencies higher than the process of interest, i.e., electronic polarization and relaxation due to vibrations and librations, while the relaxed dielectric constant ϵ_r is the value obtained after the relaxation process, i.e., dipole orientational relaxation, is complete.

Comparison of the mean-square dipole moment of the PBD melt, $\langle M(0)^2\rangle$, with that obtained by summing the mean-square dipole moment of individual chains showed agreement within statistical uncertainties in $\langle M(0)^2\rangle$ at each temperature. The same agreement was observed when the DACF for the entire system was compared with that of the polymer chains. This agreement indicates that interchain dipole–dipole correlations are unimportant in PBD and furthermore, that we can utilize the chain mean-square dipole moment in determining $\langle M(0)^2\rangle$, i.e., $\langle M(0)^2\rangle = N_{\text{chains}}\langle M_{\text{chain}}(0)^2\rangle$, where N_{chains} is the number of polymer chains (40). The chain mean-square dipole moment and DACF have significantly better statistics than the corresponding properties for the entire system. In our discussion of dielectric relaxation below, the chain mean-square dipole moments and DACFs are utilized in all calculations of the dielectric properties of the PBD melt.

B. Partial charges

Partial atomic charges for 1,4-polybutadiene were determined from fitting the electrostatic potential and dipole moments of the model compounds cis-3-hexene and 1-butene, shown in Fig. 1. Equilibrium geometries were obtained at the MP2/6-311G** level and had C_s symmetry for 1-butene and cis-3-hexene in the s^+ciss^- conformation and C_2 symmetry for cis-3-hexene in the s^+ciss^+ conformation.[44] The electrostatic potential was generated on a grid of points around each model compound using MP2/6-311G** wave functions.

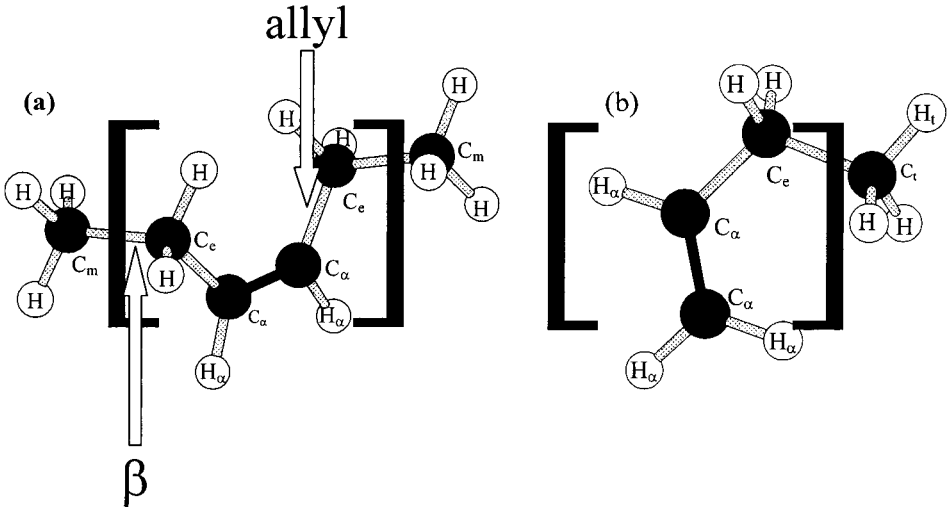

FIG. 1. Model compounds for determining partial charges for polybudadiene: (a) cis-3-hexene and (b) 1-butene. Partial charges corresponding to the indicated atom types are given in Table I. Brackets delineate the charge neutral repeat units whose partial atomic charges where used in assigning charges to the polymer. The allyl and β dihedrals for 1,4-polybutadiene are denoted.

Only those grid points no closer than 1.9 Å from any hydrogen atom and 2.5 Å from any carbon atom, with a maximum distance of 4 Å from any atom, were included in the analyses. The number of points was between 7400 and 7800 for each conformer. As partial charges obtained from these analyses were applied to the polymer, the repeat unit and termination groups for the model compounds were constrained to be charge neutral. The resulting partial atomic charges are given in Table I. This set of partial charges provides a good representation of electrostatic potential and components of the dipole moment for the model compounds.

For the purpose of calculating the DACF of the PBD melt hydrogen atoms were added to the completed united atom trajectories in the manner described previously[30] and partial atomic charges were subsequently assigned as given in Table I. This approach to inclusion of hydrogen atoms is justified by the ability of the quantum chemistry based united atom potential to reproduce conformations, dynamics and structure in the PBD melts as discussed in Sec. II above. The inclusion of partial atomic charges after completion of the molecular-dynamics simulation trajectory is justified by the very small dipole moment associated with the cis and vinyl repeat units of PBD (0.23 and 0.29 Debye for the cis and vinyl repeat units, respectively, from both quantum chemistry and our partial atomic charges). These dipole moments are sufficient to provide a very weak dielectric response of the essentially nonpolar PBD, but are insufficient to perturb structure and dynamics of the polymer significantly.

TABLE I. Partial charges for 1,4-polybutadiene model compounds.

Atom[a]	Charge (e)
C_m	+0.030
C_e[b]	+0.154
C_α[b]	−0.266
H[b]	−0.010
H_α[b]	+0.132
C_t[b]	+0.022
H_t	0.0

[a]See Fig. 1.
[b]These charges yield charge-neutral 1,4-trans, 1,4-cis and 1,2-vinyl repeat units (see Fig. 1) and were used in determination of the PBD dipole moment.

C. Dipole moment autocorrelation function

The DACF of the PBD melt for each temperature investigated is shown in Fig. 2. Since the decay at times up to 1 ps can largely be associated with bond angle vibration and dihedral librations, we determined the orientational contribution to the dipole relaxation by fitting the DACF for $t \geqslant 1$ ps with a Kohlrausch–Williams–Watts (KWW) expression with a pre-exponential factor to account for the short-time decay

$$\tilde{\Phi}(t)=A(T)\Phi(t)=A(T)\exp[-(t/\tau_{\mathrm{KWW}}(T))^{\beta(T)}]. \quad (4)$$

The resulting fits for the DACF are shown in Fig. 2, while the fitting parameters are given in Table II. The KWW equation provides a good description of the DACF for $t \geqslant 1$ ps for all temperatures. The temperature dependence of the relax-

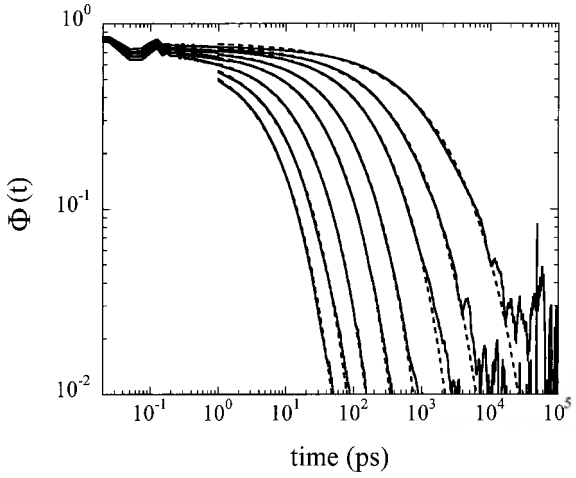

FIG. 2. Chain dipole moment autocorrelation function for the polybutadiene melt. Shown (in order of increasing relaxation time) for 500, 450, 400, 353, 323, 293, 273, and 253 K. Dashed lines are KWW fits [Eq. (4)] for $t \geqslant 1$ ps with parameters given in Table II.

TABLE II. KWW fitting parameters for the dipole moment ACF and associated dielectric properties.

T	$A(T)$	τ_{KWW} (ps)	$\beta(T)$[a]	Cell (Å)	$\langle M_{chain}(0)^2\rangle$ (Debye^2)	$\Delta\epsilon$	$\epsilon''_{max}/\Delta\epsilon$	ϵ''_{max}	ω_{max} (s^{-1})
253	0.79	1350	0.50 (0.58)	48.50	0.868	8.13×10^{-2}	0.272	2.21×10^{-2}	5.39×10^{8}
273	0.76	452	0.56 (0.65)	48.72	0.889	7.20×10^{-2}	0.301	2.18×10^{-2}	1.67×10^{9}
293	0.75	204	0.61 (0.61)	48.92	0.928	6.66×10^{-2}	0.329	2.16×10^{-2}	3.92×10^{9}
323	0.72	81.3	0.65 (0.62)	49.28	0.957	5.74×10^{-2}	0.348	1.98×10^{-2}	9.97×10^{9}
353	0.71	39.4	0.67 (0.63)	49.65	0.991	5.08×10^{-2}	0.355	1.80×10^{-2}	2.07×10^{10}
400	0.70	17.6	0.67 (0.65)	50.22	1.033	4.26×10^{-2}	0.357	1.51×10^{-2}	4.64×10^{10}
450	0.71	8.62	0.65	50.91	1.072	3.66×10^{-2}	0.346	1.26×10^{-2}	9.48×10^{10}
500	0.71	5.15	0.65 (0.71)	51.50	1.108	3.15×10^{-2}	0.346	1.09×10^{-2}	1.59×10^{11}

[a]Values in parentheses from the KWW fit to the self-correlation function for the $p=19-22$ (segmental) chain mode.

ation time τ_{DACF} for the DACF, determined as the time integral of $\Phi(t)$ given by Eq. (4), is shown in Fig. 3. A Vogel–Fulcher fit of the form

$$\ln\tau=\ln\tau_o+\frac{B}{T-T_o}, \tag{5}$$

to the τ_{DACF} values is shown in Fig. 3. The resulting Vogel–Fulcher parameters are given in Table III.

D. Dielectric relaxation strength

We utilize a value of $\epsilon_u\approx3$ as given by experimental measurements for PBD.[3,12] The relaxation strength for the dipole reorientation process in PBD is insensitive to the precise value of ϵ_u. The dielectric relaxation strength for this process for the PBD melt at each temperature is given in Table II. These relaxation strengths were determined using Eq. (3), subsequently multiplied by $A(T)$ from Table II to account for vibrational and librational effects that should be not be included in determination of the relaxation strength for the dipole reorientation process but rather included in ϵ_u. The relaxation strength at the lowest temperature is in good agreement with the value of 0.087 reported by Zorn *et al.*[12] for the combined α-β processes in a PBD of similar microstructure (trans/cis/vinyl composition).

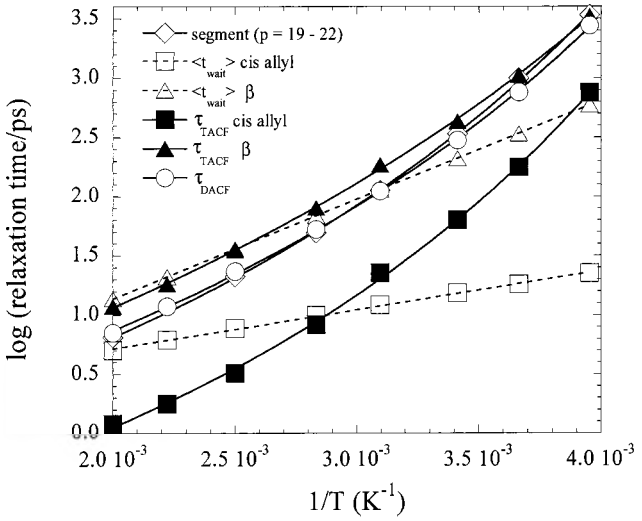

FIG. 3. Temperature dependence of principal relaxation times for the polybutadiene melt. Dashed lines are Arrhenius fits, while solid lines are Vogel–Fulcher fits [Eq. (5)] with parameters given in Table III.

E. Complex permittivity

The real and imaginary contributions to the frequency dependent complex permittivity of the PBD melt, normalized by the relaxation strength, were determined analytically by application of Eq. (1) to the KWW fits to the DACF, and are shown in Fig. 4. The maximum dielectric loss and maximum loss frequency for each temperature are given in Table II. The magnitude of the maximum loss is in good agreement with experimental data for the combined α-β process in PBD.[3,12] The maximum loss frequency is shown as a function of inverse temperature in Fig. 5, and is compared with experimental measurements. Vogel–Fulcher fits of the maximum loss frequency

$$\ln\omega_{max}=\ln\omega_o-\frac{B}{T-T_o}, \tag{6}$$

yield the Vogel–Fulcher parameters given in Table III for simulation and experiment. Very good agreement between simulation and experiment is seen, confirming the ability of the simulations to reproduce dielectric relaxation associated experimentally with the combined α-β processes. Comparing the inverse maximum loss frequency with τ_{DACF} as well as the Vogel–Fulcher parameters (B and T_o) obtained for the

TABLE III. Vogel–Fulcher parameters for various relaxation processes.

Process	Source	τ_o or ω_o	B (K)	T_o (K)
τ_{DACF}	simulation	0.38 (ps)	1100	129
dielectric ω_{max}	simulation	2.4×10^{12} (s^{-1})	1090	123
dielectric ω_{max}	Ref. 15	2.1×10^{12} (s^{-1})	1140	138
dielectric ω_{max}	Ref. 3	1.2×10^{12} (s^{-1})	770	149
τ_R (Rouse time)	simulation	98 (ps)	1140	134
η	simulation	1.9×10^{-4} (Pa-s)	1070	132
η	Ref. 47	···	1410	128
η	Ref. 10	···	770	149
$\tau_{segment}$	simulation	0.29 (ps)	1150	131
τ_{TACF} (cis allyl)	simulation	0.057 (ps)	1080	140
τ_{TACF} (β)	simulation	0.49 (ps)	1220	114
$t_{D(n)=1}$	simulation	0.62	1410	87

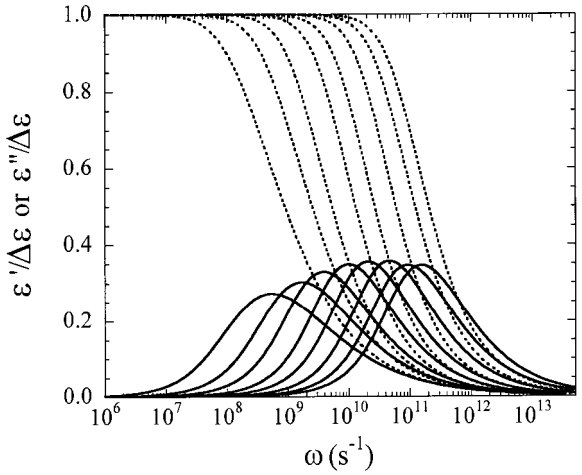

FIG. 4. Real (dotted lines) and imaginary (solid lines) components of the complex permittivity of the polybutadiene melt obtained from applying Eq. (1) to the KWW fits of the dipole moment autocorrelation function (Fig. 2). Shown (in order of decreasing maximum loss frequency) for 500, 450, 400, 353, 323, 293, 273, and 253 K.

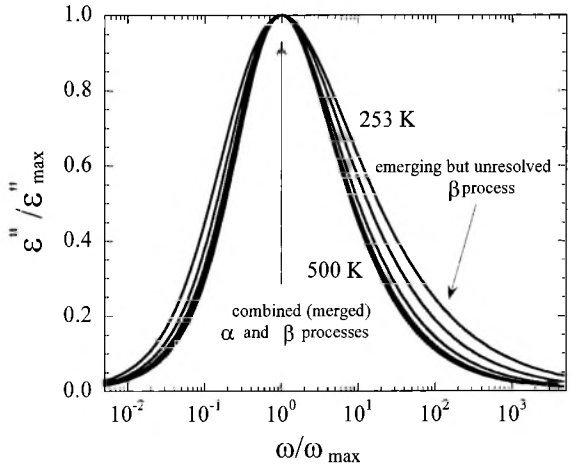

FIG. 6. Dielectric susceptibility normalized by the maximum loss and maximum loss frequency at each temperature. The peak is associated with the combined α-β relaxation in the simulation temperature range. The increasing high-frequency susceptibility with decreasing temperature is associated with the emerging β process. Data for 500, 450, 400, 353, 323, 293, 273, and 253 K are shown. The normalized susceptibility is nearly independent of temperature for the five highest temperatures.

maximum loss frequency and τ_{DACF} confirms the fundamental correspondence of these properties. Hence, in the discussions below of the relationship between dielectric relaxation, chain dynamics and conformational dynamics, we make comparisons with the DACF and its associated relaxation time τ_{DACF}.

F. Time-temperature superposition

In order to investigate the applicability of time-temperature superposition to dielectric relaxation in PBD, we have plotted $\epsilon''/\epsilon''_{\max}$ versus $\omega/\omega_{\max}$ for all temperatures investigated in Fig. 6. Time temperature superposition holds well for $T \geqslant 323$ K. For lower temperatures, the dielectric susceptibility becomes wider in frequency, with the largest effect occurring on the high-frequency flank of the susceptibility. This is an indication of an emerging, but not yet fully resolved, high-frequency β process, as discussed below.

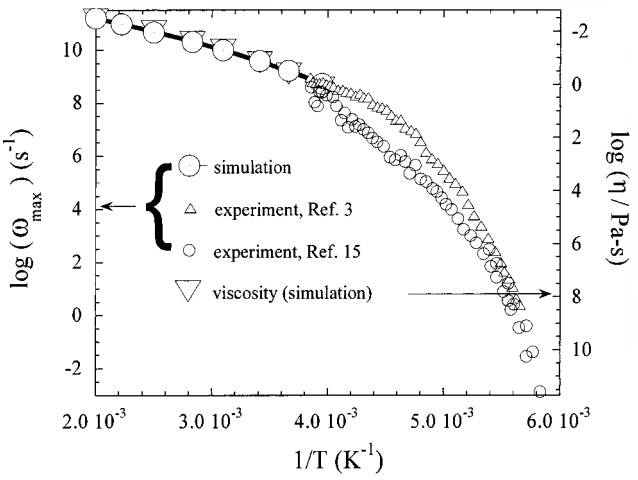

FIG. 5. Maximum dielectric loss frequency and melt viscosity for polybutadiene from simulation and experiment. The solid line is a Vogel–Fulcher fit to the simulation dielectric and viscosity data with parameters given in Table III.

Hence, in the temperature domain of the combined α-β dielectric relaxation ($T > T_b$) time-temperature superposition is only appropriate for $T \geqslant 323$ K. It is also over the temperature range $T < 323$ K that the width parameter $\beta(T)$ for the KWW fit to the DACFs becomes strongly temperature dependent, decreasing significantly (i.e., the relaxation process becomes much broader) with decreasing temperature, as can be seen in Table II. For $T \geqslant 323$ K the width parameter is independent of T within uncertainties in the fitting parameters.

IV. CHAIN RELAXATION

A. Normal mode analysis

In order to quantify the relaxation of the PBD melt chains on length scales from that of a statistical segment to that of the entire chain and relate chain relaxation to dielectric relaxation, we performed a normal mode, or Rouse mode, analysis of the polymer chain dynamics. The solution of the Rouse equation of motion is determined analytically by transformation to its eigenmodes, the Rouse modes, which are defined as[45,46]

$$X_p(t) = \sqrt{\frac{2}{N}} \sum_{n=1}^{N} \cos\left(p\pi \frac{n - 1/2}{N} \right) R_n(t) \tag{7}$$

where p is the mode index ($1 \leqslant p \leqslant N$) and $R_n(t)$ is the vector in Cartesian coordinates of united atom n at time t. The sum is over all N backbone united atoms of a PBD chain. The Rouse model yields the self-correlation function[46]

$$\langle \mathbf{X}_p(t) \cdot \mathbf{X}_p(0) \rangle = \frac{C_n l_b^2}{4 \sin^2 \dfrac{p\pi}{2N}} \exp[-t/\tau_p], \tag{8}$$

for the pth mode, where C_n is the characteristic ratio and l_b^2 is the mean-square bond length. The relaxation time for the pth mode is given by[46]

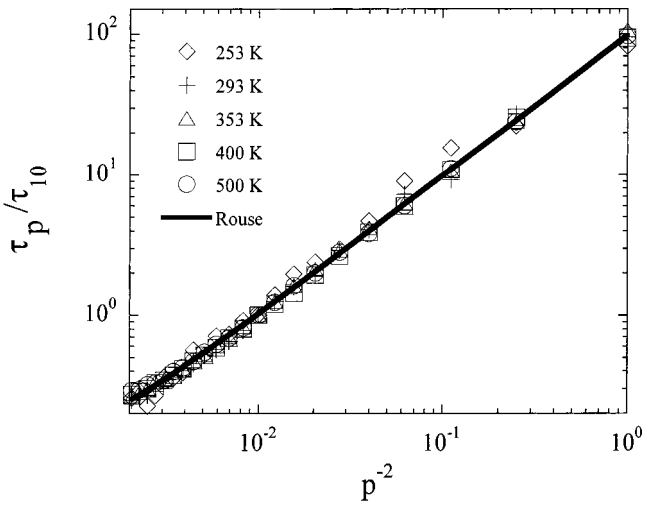

FIG. 7. Dynamic scaling of the normal modes. The solid line shows the expected scaling from Rouse theory [Eq. (9)].

$$\tau_p = \frac{\zeta C_n l_b^2}{12 k_b T} \sin^{-2}\left(\frac{p\pi}{2N}\right), \tag{9}$$

where ζ is the monomer friction coefficient. The self-correlation function was determined for $p=1-22$. A value of $p=22$ corresponds to a statistical segment of $N/22 \approx C_n \approx 5$ bonds. The mode self-correlation functions from simulation do not show single exponential decay as predicted by Eq. (8), but are well represented by a stretched exponential

$$\langle \mathbf{X}_p(t)\cdot\mathbf{X}_p(0)\rangle = \langle \mathbf{X}_p(0)\cdot\mathbf{X}_p(0)\rangle \exp[-(t/t_p)^{\beta}], \tag{10}$$

where β ranges from 1.0 for $p=1$ to around 0.6 for $p=22$. The relaxation time for each mode, given as the analytical time integral of $\exp[-(t/\tau_p)^{\beta}]$, is shown in Fig. 7 as a function of p^{-2} for each temperature investigated. Here, we have normalized the relaxation times for each temperature by the corresponding relaxation time for $p=10$. Within statistical uncertainty the normalized relaxation times show no temperature dependence for any value of p, except perhaps for the largest p values at the lowest temperatures. This indicates that time-temperature superposition is obeyed for chain dynamics for the range of temperatures investigated for chain relaxation on length scales from the entire chain down to that of the statistical segment.

For the Rouse model the relaxation time of the self-correlation function of a mode is expected to scale as $\sin^{-2}(p\pi/2N)$. As can be seen in Fig. 7, this scaling is well-followed at all temperatures. The applicability of the Rouse model to the chain relaxation in PBD allows us to use the Rouse model in predicting the viscosity. The viscosity in the Rouse model is given by[46]

$$\eta = \frac{c\pi^2 k_b T}{12}\tau_R, \tag{11}$$

where c is the concentration of polymer chains. The viscosity is shown in Fig. 5 with the temperature dependence given from experiment.[47] The Vogel–Fulcher parameters for the viscosity from simulation and experiment (for higher molecular weight PBD melts)[10,47] as well as the Rouse time τ_R[48] are given in Table III. The correspondence of the temperature dependence of the macroscopic relaxation processes (the dielectric (combined α-β) and the mechanical (viscosity) relaxation) from both simulations and experiment is apparent in Fig. 5 and Table III.

There exists an apparent disagreement between the two quoted sets of Vogel–Fulcher parameters obtained from experimental viscosity measurements, and to a lesser extent, between our Vogel–Fulcher fits to the two sets of experimental dielectric data shown in Fig. 5. This discrepancy has two sources. First, as can be seen for the dielectric data, there are differences in the experimental data themselves. Additionally, within the temperature range of the experimental data, particularly for the viscosity data which cover a narrower range than the dielectric data, the Vogel–Fulcher parameters are not unique. The quality of fit changes little within a range of values for the Vogel–Fulcher parameters, indicating a high degree of correlation between the T_o and B parameters. Consequently, over the temperature range of the experimental viscosity data, the two sets of experimental Vogel–Fulcher parameters and our set from simulation yield similar temperature dependence of the viscosity.

B. Relationship between chain dynamics and dielectric relaxation

Figure 3 shows a comparison of the DACF and segmental relaxation times. The latter is given as the average of the relaxation times for the $p=19-22$ normal modes. The DACF relaxation time τ_{DACF} is nearly identical to the segmental relaxation time at all temperatures, indicating that dielectric relaxation is localized to the length scale of a statistical segment, i.e., about five bonds. This similarity is further manifested when the Vogel–Fulcher fits of the DACF and segmental relaxation times, given in Table III, are compared. Since the 1,4-cis units make up the majority of the dipole moment of the PBD chain, the correspondence between DACF and segmental relaxation times allows us to assign dielectric relaxation in PBD to the reorientation of the 1,4-cis units that results primarily from dynamics of bonds (dihedrals) within two bonds on either side of the cis double bond, i.e., primarily from dynamics of the immediately neighboring cis allyl and β dihedrals.

Above we noted that for dielectric relaxation time-temperature superposition is valid only for $T \geqslant 323$ K, while for chain relaxation it appears to be valid for all temperatures investigated. Detailed analysis of the width parameter (β) for the segmental relaxation, given as the average of values obtained from KWW fits to the $p=19-22$ normal modes, given in Table II, shows that on the segmental length scale the width parameter may be decreasing at the lowest temperatures investigated, thereby indicating a breakdown of time-temperature superposition. Simulations at lower temperatures are needed to fully resolve this issue.

V. CONFORMATIONAL DYNAMICS

Conformational dynamics were monitored by investigating both the rates of conformational transitions and the decay of the torsional autocorrelation function (TACF) for cis allyl

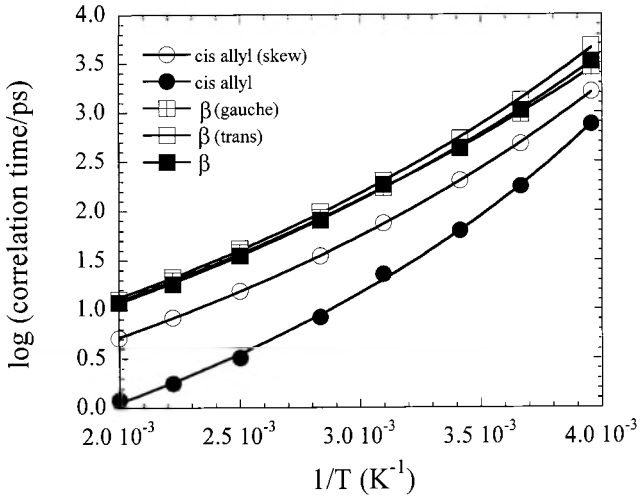

FIG. 8. A comparison of torsional autocorrelation times obtained from the $P(t)$ torsional autocorrelation function [Eq. (12), closed symbols] and the $p(t)$ torsional autocorrelation function [Eq. (13), open symbols] for β and cis allyl dihedrals as a function of temperature. Solid lines are Vogel–Fulcher fits [Eq. (5)] to the torsional autocorrelation times.

and β dihedrals.[49] The former was analyzed in terms of the distribution of waiting times for dihedral transitions. The conformational state of each dihedral was determined every picosecond, and a transition (cis$\leftrightarrow s^{\pm}+s^{+}\leftrightarrow s^{-}$ transitions for cis allyl dihedrals and $t\leftrightarrow g^{\pm}+g^{+}\leftrightarrow g^{-}$ transitions for the β dihedrals) was considered to occur whenever the state of the dihedral changed. The inverse mean rate of dihedral transitions for a given type (cis allyl or β) is given by the mean waiting time $\langle t_{\mathrm{wait}}\rangle$ between transitions of dihedrals of that type. The TACF was determined as in our previous work[31] using the relationship

$$P_i(t)=\frac{\langle\cos(\phi_i(t))\cos(\phi_i(0))\rangle-\langle\cos(\phi_i(0))\rangle^2}{\langle\cos^2(\phi_i(0))\rangle-\langle\cos(\phi_i(0))\rangle^2}, \quad (12)$$

where the subscript indicates the kind of dihedral and $\phi_i(t)$ is the dihedral angle of a dihedral of type i at time t and the brackets denote an ensemble average over all dihedrals of type i. We also investigated the behavior of the TACF defined alternatively as[50]

$$p_{i\alpha}(t)=\frac{\langle H_{i\alpha}(t)H_{i\alpha}(0)\rangle-\langle H_{i\alpha}\rangle^2}{\langle H_{i\alpha}^2\rangle-\langle H_{i\alpha}\rangle^2}, \quad (13)$$

where the subscript i denotes the kind of dihedral and the subscript α denotes the state of the dihedral (gauche or trans for β dihedrals, skew or cis for allyl dihedrals). The function $H_{i\alpha}(t)$ has a value of unity for a particular dihedral of type i if it is in state α at time t, otherwise $H_{i\alpha}(t)$ has a value of zero. A comparison of the correlation times obtained by the analytical time integral of KWW fits to $P_i(t)$ (see below) and $p_{i\alpha}(t)$ as a function of temperature for β and cis allyl dihedrals is shown in Fig. 8. The torsional autocorrelation times obtained from $P(t)$ for the β dihedral are nearly indistinguishable from those obtained from $p(t)$ for the gauche and trans states of the β dihedral. The torsional autocorrelation time from $P(t)$ for the cis allyl dihedral is somewhat shorter than that obtained from $p(t)$ for the skew state of the cis allyl dihedral (the cis population of the cis allyl dihedral is negligible). For the trans allyl (not shown), agreement between correlation times obtained from $P(t)$ and $p(t)$ is intermediate to that found for the β and cis allyl dihedrals. For all dihedrals, the Vogel–Fulcher parameters B and T_o [Eq. (5)] obtained from fitting the temperature dependence of the correlation times from $P(t)$ and $p(t)$ were found to be essentially identical. Hence, for the purpose of comparing the time scale of dielectric relaxation and conformational dynamics, as well as their non-Arrhenius temperature dependence (see below), the alternative definitions of the torsional autocorrelation function given by Eqs. (12) and (13) are equivalent. In this paper we utilize Eq. (12) in our analysis of conformational dynamics.

A. Conformational dynamics and dielectric relaxation

The TACFs for the cis allyl and β dihedrals were found to be reasonably well represented by a KWW fit function of the form given by Eq. (4) for $t\geqslant 1$ ps. Integration of the resulting KWW equations yielded the torsional autocorrelation times τ_{TACF} shown in Fig. 3 as a function of inverse temperature for the cis allyl and β dihedrals. Also shown is $\langle t_{\mathrm{wait}}\rangle$ for these dihedrals. Figure 3 reveals that the time scale for dielectric relaxation (τ_{DACF}) lies intermediate to the time scales for τ_{TACF} of the cis allyl and β dihedrals. Furthermore, the Vogel–Fulcher parameters (Table II) for cis allyl and β dihedral τ_{TACF}'s are consistent with those for τ_{DACF}. These correspondences provide a clear connection between the microscopic process of conformational dynamics and the macroscopic process of dielectric relaxation, indicating that conformational transitions of these dihedrals are primarily responsible for dielectric relaxation in PBD through reorientation of the polar 1,4-cis repeat units, as anticipated based upon comparison of dielectric relaxation and normal-mode dynamics.

B. Distribution of waiting times and homogenization of conformational dynamics

It can be clearly seen in Fig. 3 that while the τ_{TACF}'s for the cis allyl and β dihedrals show non-Arrhenius temperature dependence well represented by the Vogel–Fulcher equation, $\langle t_{\mathrm{wait}}\rangle$ exhibits Arrhenius temperature dependence over the range of temperatures investigated. This disconnect between the TACF (and for PBD, the DACF) and the mean rate (inverse of the mean waiting time) of conformational transitions has been observed previously[31,51] in simulations of polymer melts and solutions. As we noted in previous work,[31] the mean waiting time is more dependent upon fast events while the decay of the TACF depends upon the slowest events—the latter cannot decay until all dihedrals have visited all conformational state with equilibrium probability.

One possibility for the decreasing efficiency of conformational transitions at effecting dihedral and dielectric relaxation in PBD with decreasing temperature is the increasingly self-correlated nature of conformational transitions with decreasing temperature observed in polymer melts and solutions.[31,51] Self-correlated transitions are frequently immediate or near-immediate back jumps between two conformational states and as such are relatively ineffective in promoting decay of the TACF, which requires visitation of all

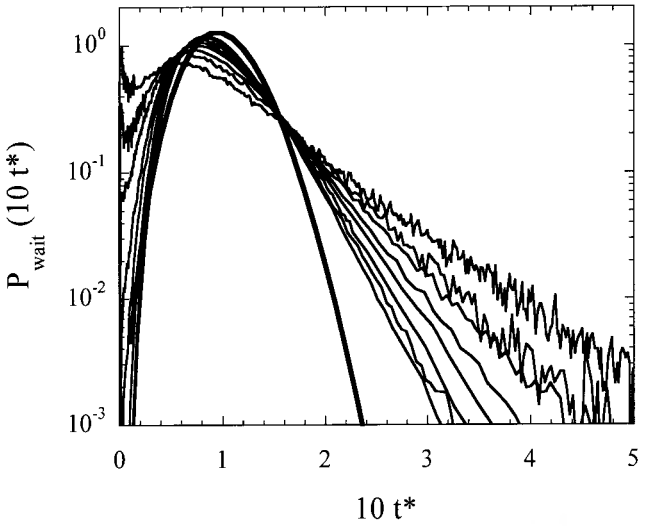

FIG. 9. Distribution of waiting times for ten transitions of a β dihedral. Shown (in order of increasing heterogeneity for 500, 450, 400, 353, 323, 293, 273, and 253 K). The heavy solid line shows expected behavior for a homogeneous system (Poisson) distribution. Corresponding dispersions $D(n=10)$ are 0.1 (Poisson), 0.146, 0.159, 0.178, 0.208, 0.241, 0.313, 0.388, and 0.599.

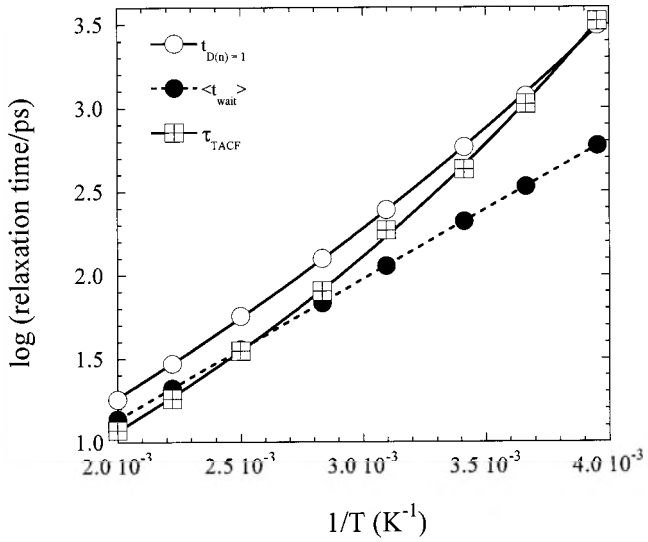

FIG. 10. Comparison of waiting, homogenization, and the torsional autocorrelation times for β dihedrals.

conformational states by each dihedral. Self-correlated transitions are characterized by short waiting times between consecutive jumps and as such show up as the short-time peak in Fig. 9 at lower temperatures. This figure shows the distribution of reduced ($t^* = t/\langle t_{\text{wait}} \rangle$) times for a β dihedral to undergo ten transitions (i.e., the waiting time distribution for ten dihedral transitions) along with the expected Poisson distribution for a homogeneous system, i.e., a system where all transitions are uncorrelated and all dihedrals experience the same probability for a transition during any time window.[31] The time distribution approaches the Poisson distribution at high temperatures, indicating relatively homogeneous dihedral dynamics. At lower temperatures, the probability for the ten transitions to occur quickly (i.e., the probability of a short waiting time) on the reduced time scale increases dramatically. In addition, with decreasing temperature there is increasing probability for a dihedral to take much longer than the average time to undergo the ten transitions, i.e., there is an increased probability for some dihedrals to experience much slower than average dynamics. In summary, we observe that conformational transitions are becoming increasingly heterogeneous as temperature decreases, with increasing probability of relatively fast dihedrals undergoing rapid, self-correlated transitions and increasing probability of relatively quiescent dihedrals with very long waiting times between transitions.

We characterize the distribution of waiting times for various values of n, the number of transitions, such as shown in Fig. 9 for $n=10$, by their normalized dispersion $D(n) = \sigma^2(n,T)/n^2$, where σ is the second central moment of the distribution. For all temperatures $D(n)$ was observed to decrease with increasing n, i.e., the distribution of waiting times becomes relatively narrower with increasing n. This indicates that the conformational dynamics are becoming more homogeneous when averaged over time, i.e., that initially fast jumping dihedrals eventually become slow for a period, and initially slow dihedrals become faster. This is in contrast to a recent MD simulation study of conformational dynamics in a poly(ethylene) glass,[52] where the normalized dispersion was found to be independent of n, indicating no homogenization of conformational dynamics.

For a given value of n, $D(n)$ was found to increase dramatically with decreasing temperature (see for example Fig. 9 for $n=10$), particularly for the lowest temperatures investigated. The dispersion is strongly influenced by the increasing probability of slow dihedrals with decreasing temperature such as indicated by the long-time tail in Fig. 9. We can take into account the influence of the increasing dispersion (higher probability of very fast (correlated) and very slow dihedrals) on conformational dynamics by comparing the times at which $D(n) = \text{constant}$ for each temperature. We have done this for $D(n)=1$. For a system with homogeneous conformational dynamics $D(n)=1$ occurs at $n=1$, which is equivalent to a time $t_{D(n)=1} = n\langle t_{\text{wait}} \rangle = \langle t_{\text{wait}} \rangle$. Furthermore, since $\langle t_{\text{wait}} \rangle$ corresponds to the relaxation time τ_{TACF} of the TACF for a homogeneous system,[31] it is reasonable to anticipate that $t_{D(n)=1}$ will be correlated with τ_{TACF} for the real (heterogeneous) melts. The values $t_{D(n)=1}$ for each temperature are shown in Fig. 10. While still not as strongly diverging as τ_{TACF}, τ_{DACF} or the viscosity, the "homogenization time" given by $t_{D(n)=1}$ shows a much stronger temperature dependence than $\langle t_{\text{wait}} \rangle$ and is in much better agreement with these relaxation times and their temperature dependence, as can further seen by comparing Vogel–Fulcher parameters for $t_{D(n)=1}$ with those for τ_{TACF}, τ_{DACF}, and the viscosity in Table III. We believe this correspondence demonstrates that the temperature dependence of the microscopic conformational relaxation (TACF), and hence the macroscopic dielectric and mechanical relaxations, is strongly tied to the increasingly heterogeneous nature of conformational dynamics, particularly the emergence of very slow dihedrals, with decreasing temperature, and that these relaxations reflect the time scale for homogenization of conformational

dynamics, i.e., the time scale on which most dihedrals undergo something like the mean number of transitions.

VI. CONCLUSIONS AND FUTURE WORK

We have presented MD simulations of a chemically realistic model of 1,4-polybutadiene over a wide temperature range in the melt. Over this range of temperatures the dielectric α and β relaxations are still merged. Comparing the static and dynamic behavior of the chain average dipole moment and the box dipole moment we established that there are no intermolecular dipole correlations in the PBD melt. This allows us to determine the dielectric response of the melt from the behavior of the chain dipole moment with good statistical accuracy. We find that the strength of the dielectric response as well as the temperature dependence of the maximum loss frequency, including its non-Arrhenius character, for the combined α-β relaxation from simulation are in excellent agreement with available experimental data.

In order to determine the length scale of polymer chain relaxation involved in effecting dipolar relaxation, we compared the dipolar relaxation with the chain relaxation on length scales ranging from the statistical segment to the entire chain as quantified by the Rouse modes. The time autocorrelation functions of the modes display a KWW behavior with a stretching that increases with the mode number, which differs from the Rouse theory expectations. However, the integrated relaxation times of the modes follow the Rouse prediction for scaling with mode number. Furthermore, dielectric relaxation and chain relaxation on all length scales follow the same Vogel–Fulcher behavior within the uncertainty of the parameter determination. Additionally, using the Rouse theory for calculation of the melt viscosity we again get Vogel–Fulcher parameters for the viscosity in good agreement with experimental results. Finally, comparing the time scale of the dipolar relaxation with those of the Rouse modes we can establish that the dipolar relaxation corresponds to the relaxation of one statistical segment in the PBD chain, or about five backbone bonds (dihedrals).

At 323 K and above, dielectric relaxation, as determined by normalized [to $\omega_{\max}(T)$] susceptibility, and the chain relaxation, as monitored by the normalized [to $\tau_{10}(T)$] relaxation times, obey the time-temperature superposition principle. For lower temperatures we observe the appearance of excess high frequency intensity in the combined α-β dielectric susceptibility signaling the emergence of the β process. Some breakdown of time-temperature superposition for the chain modes also may occur on the statistical segment length scale at the lowest temperatures. While our simulations are still above the dielectric bifurcation temperature $T_b \approx 200$ K,[15] and hence a dielectric β process is not expected to be resolvable in either our simulations or in experiments in this temperature range, signatures of the β process above the dielectric T_b have been seen in neutron scattering studies of PBD.[3] Specifically, in this temperature range, neutron spin echo experiments performed at the momentum transfer given by the position of the second, intramolecular peak in the static structure factor yielded an Arrhenius dependence of the corresponding relaxation time with an activation energy close to that of the dielectric β process.

Examination of conformational dynamics yielded insight into the microscopic mechanism of dielectric and mechanical relaxation in the PBD melt. The relaxation of a 1,4-cis segment, which carries the main dipole moment for PBD, comes about by transitions in the neighboring dihedrals. Consequently the dielectric relaxation time is bracketed by that of the autocorrelation functions for the allyl cis and β dihedrals. The mean rates of conformational transitions for both dihedrals follow an Arrhenius temperature dependence with activation energies given by the respective rotation barriers. In order to understand the Vogel–Fulcher type behavior of the torsional autocorrelation functions and hence that of the combined α-β dielectric and mechanical relaxations, we must explain the divergence of the time scale of these relaxations and that of the conformational transitions with decreasing temperature. When chemical equivalent dihedrals exhibit heterogeneous conformational dynamics, the mean transition rate is most sensitive to the fast moving torsions whereas the torsional autocorrelation function is more sensitive to the very slow torsions. To quantify the heterogeneity in the conformational dynamics we measured the distribution of waiting times for a given number of transitions. Compared to the Poisson behavior of independent random events, we observed an increase in probability for very short waiting times, which is due to correlated transitions, and a long time tail due to very slow dihedrals. At high temperatures the distribution approaches the expected Poisson behavior. Utilizing the dispersion as a measure to quantify the excess width of the waiting time distribution allows for the definition of a "homogenization" time scale on which the dispersion is equal to that associated with a homogeneous (Poisson) system on the time scale of relaxation time of the torsional autocorrelation function. This homogenization time scale shows a clear non-Arrhenius temperature dependence. We, therefore, conjecture that the time scale for the macroscopic dielectric and mechanical relaxations, i.e., the α time scale, is mirroring the homogenization time for the basic local motion mechanism, i.e., the conformational transitions. This supposition is supported by recent simulation studies of a polymer below T_g, where it was found that conformational dynamics did not homogenize on the time scale of the simulations.[52]

In extending this analysis to lower temperatures, especially the α-β merging temperature, we expect to be able to provide a mechanistic understanding of the microscopic motions associated with the β process, and a much better understanding of the relationship between the α and β relaxations. The quality of our model will also allow us to make quantitative comparisons with the experiment, particularly dielectric and neutron scattering studies, in the $200\ \text{K} \leqslant T \leqslant 253\ \text{K}$ range, as well to test the predictions of mode-coupling theory for PBD in this temperature range. The ability to simulate the melt in this temperature range will also allow us to address fundamental questions associated with experimentally observed dynamic heterogeneity in polymer melts[53] in the temperature range $T \leqslant 1.2T_g$ (220 K for PBD). Work to generate equilibrated starting melt configurations in the merging temperature regime is currently under way. It is necessary to study the relaxation behavior for equilibrated

systems because frozen in high-temperature structures can lead to orders of magnitude decrease in apparent relaxation times due to physical aging effects.

ACKNOWLEDGMENTS

One of the authors (W.P.) acknowledges funding through the German Science Foundation under Grant No. DFG Pa473/3-2. G.S. acknowledges support of the ACS-PRF through Grant No. G7-301 and the University of Utah Center for the Simulation of Accidental Fires and Explosions (C-SAFE), funded by the Department of Energy, Lawrence Livermore National Laboratory, under subcontract B341493.

[1] *Dynamics of Disordered Materials*, edited by A. J. Dianoux, W. Petry, and D. Richter (North-Holland, Amsterdam, 1993).
[2] G. P. Johari and M. Goldstein, J. Chem. Phys. **53**, 2372 (1970).
[3] A. Arbe, D. Richter, J. Colmenero, and B. Farago, Phys. Rev. E **54**, 3853 (1996).
[4] J-L. Viovy, L. Monnerie, and F. Merola, Macromolecules **18**, 1130 (1985).
[5] R. Dejean de la Batie, F. Laupretre, and L. Monnerie, Macromolecules **22**, 122 (1989).
[6] A. Guillermo, R. Dupeyre, and J. P. Cohen-Addad, Macromolecules **23**, 1291 (1990).
[7] E. Rüssler, A. Sokolov, P. Eiermann, and U. Warschewske, Physica A **201**, 237 (1993).
[8] S. Wartewig, I. Alig, F. Stieber, and G. Fytas, J. Chem. Phys. **80**, 172 (1989).
[9] I. Alig, F. Stieber, and S. Wartewig, J. Non-Cryst. Solids **131**, 808 (1991).
[10] R. Zorn, G. B. McKenna, L. Willner, and D. Richter, Macromolecules **28**, 8552 (1995).
[11] S. Poshyachinda, H. G. M. Edwards, and A. F. Johnson, Polymer **37**, 5171 (1996).
[12] R. Zorn, F. I. Mopsik, G. B. McKenna, L. Willner, and D. Richter, J. Chem. Phys. **107**, 3645 (1997).
[13] D. Fioretta, L. Palmieri, G. Socino, and L. Verdini, Phys. Rev. B **50**, 605 (1994).
[14] A. P. Sokolov, U. Buchenau, W. Steffan, B. Frick, and A. Wischnewski, Phys. Rev. B **52**, 9815 (1995).
[15] A. Aouadi, M. J. Lebon, C. Dreyfus, B. Strube, W. Steffen, A. Patkowski, and R. M. Pick, J. Phys.: Condens. Matter **9**, 3803 (1997).
[16] R. D. Deegan and S. R. Nagel, Phys. Rev. B **52**, 5653 (1995).
[17] D. Richter, B. Frick, and B. Farago, Phys. Rev. Lett. **61**, 2465 (1988).
[18] B. Frick, D. Richter, and C. Ritter, Europhys. Lett. **9**, 557 (1989).
[19] B. Frick, B. Farago, and D. Richter, Phys. Rev. Lett. **64**, 2921 (1990).
[20] T.K. Kanaya, K. Kaji, and K. Inoue, Macromolecules **24**, 1826 (1991).
[21] B. Frick, R. Zorn, D. Richter, and B. Farago, J. Non-Cryst. Solids **131**, 169 (1991).
[22] D. Richter, R. Zorn, B. Farago, B. Frick, and L. J. Fetters, Phys. Rev. Lett. **68**, 71 (1992).
[23] U. Buchenau, C. Schönfeld, D. Richter, T. Kanaya, K. Kaji, and R. Wehrmann, Phys. Rev. Lett. **73**, 2344 (1994).
[24] R. Zorn, D. Richter, B. Frick, and B. Farago, Physica A **201**, 52 (1993).
[25] R. Zorn, A. Arbe, J. Colmenero, B. Frick, D. Richter, and U. Buchenau, Phys. Rev. E **52**, 781 (1995).
[26] A. Arbe, U. Buchenau, L. Willner, D. Richter, B. Farago, and J. Colmenero, Phys. Rev. Lett. **76**, 1872 (1996).
[27] R. Zorn, T. Kanaya, T. Kawaguchi, D. Richter, and K. Kaji, J. Chem. Phys. **105**, 1189 (1996).
[28] A. Arbe, D. Richter, J. Colmenero, and B. Farago, Physica B **234**, 437 (1997).
[29] D. Richter, J. Phys.: Condens. Matter **8**, 9176 (1997).
[30] G. D. Smith, W. Paul, M. Monkenbusch, L. Willner, D. Richter, X. H. Qiu, and M.D. Ediger, Macromolecules **32**, 8857 (1999).
[31] G. D. Smith, O. Borodin, D. Bedrov, W. Paul, X. H. Qiu, and M. D. Ediger, Macromolecules **34**, 5192 (2001).
[32] G. D. Smith and W. Paul, J. Phys. Chem. A **102**, 1200 (1998).
[33] G. D. Smith, W. Paul, M. Monkenbusch, and D. Richter, Chem. Phys. **261**, 61 (2000).
[34] G. D. Smith, W. Paul, M. Monkenbusch, and D. Richter, J. Chem. Phys. **114**, 4285 (2001).
[35] O. Byutner and G. D. Smith, Macromolecules **34**, 134 (2001).
[36] O. Byutner and G. D. Smith, J. Polym. Sci., Part B: Polym. Phys. **39**, 3067 (2001).
[37] O. Byutner and G. D. Smith, Macromolecules **35**, 3769 (2002).
[38] At 253 K the Rouse time is too long to allow equilibration for multiple Rouse times.
[39] W. G. Hoover, Phys. Rev. A **31**, 1695 (1985)
[40] G. J. Martyna, M. Tuckerman, D. J. Tobias, and M.L. Klein, Mol. Phys. **87**, 1117 (1996).
[41] D. M. F. Edwards, P. A. Madden, and I. R. McDonald, Mol. Phys. **51**, 1141 (1984).
[42] J. G. Kirkwood, J. Chem. Phys. **7**, 911 (1939).
[43] G. D. Smith, in *Sub-glass Dielectric Relaxations in Polar Polymers*, Ph.D. thesis, University of Utah, 1990.
[44] See Ref. 32 for complete description of conformer notations for PBDel compounds.
[45] W. Paul, G. D. Smith, and D. Y. Yoon, Macromolecules **30**, 7772 (1997): G. D. Smith, W. Paul, D. Y. Yoon, A. Zirkel, J. Hendricks, D. Richter, and H. Schober, J. Chem. Phys. **107**, 4751 (1997).
[46] A. Kopf, B. Dünweg, and W. Paul, J. Chem. Phys. **107**, 6945 (1997).
[47] G. C. Berry and T. G. Fox, Adv. Polym. Sci. **5**, 261 (1968).
[48] Because of better statistics for the higher p modes compared with the $p=1$ mode, and the p^{-2} dynamic scaling shown in Fig. 7, the Rouse time was determined at each temperature as $\tau_R = 100\,\tau_{10}$, where τ_{10} is the relaxation time for the $p=10$ normal mode.
[49] Because of the strong connection between dielectric relaxation and the dynamics of the cis allyl and β dihedrals, results are reported only for these dihedrals. Other dihedrals, e.g., the trans allyl, behaved in a qualitatively similar manner to these.
[50] D. Brown and J. H. R. Clarke, J. Chem. Phys. **92**, 3062 (1990).
[51] O Borodin and G. D. Smith, Macromolecules **33**, 2273 (2000).
[52] W. Jin and R. H. Boyd, Polymer **43**, 503 (2002).
[53] M. D. Ediger, Annu. Rev. Phys. Chem. **51**, 99 (2000).